Quantitative evaluation of sea−ice disaster in Bohai Sea based on GOCI and Sentinel−1

LIU Meijie[1, 2], WANG Jin[1, 2], ZHONG Shilei[1], YOU Hao[1], LIANG Qi[1], CHEN Ting[1], LI Wenbo[1], YANG Xiaohan

1. *Sohool of Physicat Sciences, Qingdao University, Qingdao,* 266071*, China*;
2. *First Institute of Oceanography, First Institute of Oceanography, Ministry of Natural Resources of China, Qingdao,* 266061*, China*

Abstract: The Circum-Bohai-Sea Region is an important economic zone of China. The sea ice, which occurs at each winter, is the major marine hazard of the Bohai Sea. As a result, it is very important to evaluate the damage effects quantitatively in this region, which is seldom studied and analyzed systematically using long-time-series data. In this paper, the sea-ice disaster in the Bohai Sea is evaluated quantitatively based on the Sentinel-1 and GOCI. For different hazard-bearing bodies of the marine transportation and the offshore constructions, different sea-ice-hazard indexes are defined, which can be applied to analyze the sea-ice disaster quantitatively in the Bohai Sea, including the annual and inter-annual variations in the period from 2011 to 2017. The analysis results can provide the reference of the sea-ice monitoring in the Bohai Sea.

Key words: the Bohai Sea, sea-ice disaster, the quantitative evaluation, Sentinel-1, GOCI.

Citation format: Liu M J,Wang J,Zhong S L,You H,Liang Q,Chen T,Li W B and Yang X H. 2020. Quantitative evaluation of sea−ice disaster in Bohai Sea based on GOCI and Sentinel−1. Journal of Remote Sensing (Chinese). 24(S1): 118−125

1 INTRODUCTION

The Bohai Sea and its coastal regions have significant economic value for China, which account for about one fifth of China's GDP (Zhang, *et al*., 2016). Sea ice in the Bohai Sea not only influences the regional climate of the north china, but also poses a great threat to the marine transportation and offshore constructions (Shi, *et al*., 2012a, 2012b), which leads to severe economic losses in China (Yang, 2000; Liu, *et al*., 2015). For example, in the winter of 2009 to 2010, the sea-ice disaster caused direct economic losses amounting to several billion dollars (Su, *et al*., 2012a, 2012b). Therefore, it is very important to monitor, analyze and evaluate the sea-ice and its damaging effects (Xie, *et al*., 2006; Su, *et al*., 2012).

The early sea-ice monitoring in the Bohai Sea mainly depended on the field measurements, which is time consuming, and limited in space and time (Yang, 2000; Xu, *et al*., 2012). So far the scientific community has devoted many efforts to the sea-ice monitoring based on the satellite remote sensing (Luo, *et al*., 2004; Gu, *et al*., 2013; Liu, *et al*., 2014). SAR and optical remote sensing, which are the two main methods for sea-ice remote sensing, have their own advantages, respectively (Liu, *et al*., 2015). The sea ice can be identified and classified visually by optical images. However, the images tend to be influenced by the atmospheric attenuation and weather conditions (Shi, *et al*., 2012a, 2012b). In comparison, SAR can penetrate clouds and rain to achieve the all-time and all-weather observations. However, the SAR images are not intuitive (Luo, *et al*., 2004; Liu, *et al*., 2013).

In this paper, the quantitative evaluation of the sea-ice disaster in the Bohai Sea has been studied based on both the optical images of GOCI and the SAR images of Sentinel-1. For different hazard-bearing bodies of the marine transportation and the offshore constructions, the different sea-ice-hazard indexes have been defined using the sea-ice parameters including the concentration, thickness, and velocity. The sea-ice parameters can be extracted by the existing methods using the GOCI and Sentinel-1 data. Then, the sea-ice-hazard indexes are applied to analyze the space-time distribution of the sea-ice disaster quantitatively in the Bohai Sea from 2011 to 2017.

2 RESEARCH AREA AND DATA SOURCES

2.1 Research area

The Bohai Sea in china (Fig. 1) is a semi-enclosed sea of the continental shelf with the range of 37°07N′—41°00′N, and 117°35E′—122° 15′, and it is the southernmost frozen sea in the Northern Hemisphere.

Received: 2019-10-21; **Accepted:** 2020-04-16

Foundation: National Natural Science Foundation of China (No. 41976173); Shandong Provincial Natural Science Foundation, China (NO. ZR2019MD016); Fund of Oceanic telemetry Engineering and Technology Research Center, Ministry of Natural Resources of china (No.2016003); Basic Scientific Fund for National Public Research Institutes of China (No.2014G31).

First author biography: LIU Meijie (1978—), female, lecturer, Her research interest is ocean remote sensing, E-mail: liu_meijie@163.com

Corresponding author biography: WANG Jin(1979—), male, lecturer, Her research interest isocean remote sensing, E-mail: feiyu_wj@163.com

The sea ice in the Bohai Sea appears in winter due to the frequent occurrence of strong winter currents, which belongs to first-year ice from November to March of the following year and develops more heavily from January until February (Wu, *et al*., 2006; Yuan, *et al*., 2012).

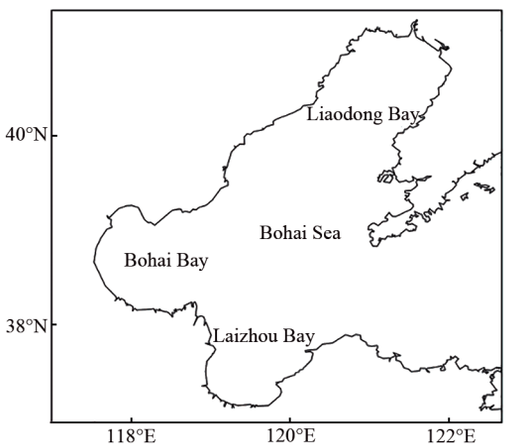

Fig.1 Location of the Bohai Sea in china

2.2 Data sources

(1) *Sentinel-1 data*

The Sentinel-1 mission is a constellation consisting of two polar-orbiting satellites (Sentinel-1A\B, Fig. 2), operating day and night performing C-band synthetic aperture radar imaging, enabling them to acquire imagery regardless of the weather (Sentinel-1, 2016), and providing single- and dual-polarization data. The Sentinel-1 data in the paper is from 2014 to 2017.

(2) GOCI *data*

GOCI (Geostationary Ocean Color Imager), which is a payload of COMS satellite launched in Korea in 2009, is the first geostationary sensor in the world. GOCI covers the whole Bohai Sea completely with a spatial resolution of about 500 m of 8 images for one daytime (Fig. 3). The GOCI data in the paper is Level-1B data with little cloud from 2011 to 2017 provided by the Korea Ocean Satellite Center (KOSC).

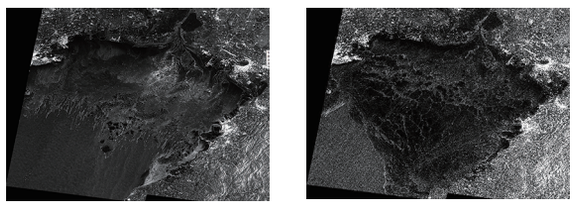

(a) 2016-01-16 (b) 2016-01-28

Fig.2 Sentinel-1 images

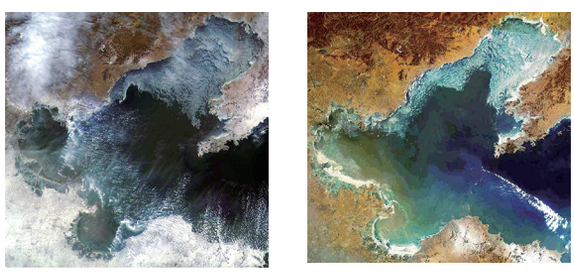

(a) 2013 02-08 (b) 2016-02-02

Fig.3 The GOCI images Red channel: band 5; green channel: band 4; blue channel: band 3

3 SEA-ICE PARAMETERS RETRIEVAL

Sea-ice parameters should be inversed for the sea-ice-hazard evaluation, which include the sea-ice concentration, thickness and velocity.

According to the Sea-ice-hazard Emergency Plan, Sea-ice-hazard Bulletin from the State Oceanic Administration, People's Republic of China (SOAPRC), the sea-ice parameters can be divided into four grades, which is shown in Table 1.

Table 1 The grades of the sea-ice parameters

Sea-ice parameters	Grade 1 Non hazard	Grade 2 Low hazard	Grade 3 Mild hazard	Grade 4 Severe hazard
Concentration	0—15 %	15—50 %	50—80 %	80—100 %
Thickness	0—0.1 m	0.1—0.2 m	0.2—0.3 m	>0.3 m
Velocity	0—0.2 m/s	0.2—0.4 m/s	0.4—0.6 m/s	>0.6 m/s

3.1 Sea-ice thickness

The sea-ice thickness (H_i) is retrieved using the sea-ice optical information of GOCI in the Bohai Sea (Liu, *et al*., 2016; Liu, 2016). The sea-ice shortwave albedo changes with the sea ice thickness as (Grenfell, *et al*., 1984)

$$\alpha_{short} = \alpha_{max}\,(1-k\exp(-\mu_{\alpha}H)) \quad (1)$$

where, α_{short} is the sea-ice shortwave broadband albedo; α_{max} is the sea-ice albedo at the infinite thickness, which is taken as 0.7 in the Bohai Sea; k is the correlation coefficient $k=1-\alpha_{sea}/\alpha_{max}$; α_{sea} is the albedo of the sea-water with the value of 0.06; and μ_{α} is the attenuation coefficient of the albedo with the value of 1.209 (Su, *et al*., 2012a). The equation of α_{short} calculated by 8 visible infrared spectra of GOCI was proposed as (Liu, 2016; Ryu, *et al*., 2012; Kim, *et al*., 2014)

$$\alpha_{short} = -0.136\alpha_1-0.270\alpha_2+1.409\alpha_3-0.328\alpha_4-0.081\alpha_5 +0.620\alpha_6-0.147\alpha_7-0.0268\alpha_8-0.046 \quad (2)$$

The results are shown in Fig. 4 in Orthographic projection (unit: m).

3.2 Sea-ice concentration

The sea ice and the sea water are detected based on Sentinel-1 and GOCI using the sea-ice optical and microwave features, which is used to calculate the sea-ice concentration (C_i) in the Bohai Sea.

(1) *Sea-ice concentration calculated by Sentinel-1*

The sea ice and the sea water are identified using the threshold method based on the Sentinel-1 (Zhang, *et al*., 2016). In the classi-

fied results of the Sentinel-1 images, the pixels classified to the sea ice are set to 1; the other pixels classified to the sea water are set to 0. The resolution of the Sentinel-1 images is reduced to that of the GOCI images which is 500 m, then the sea-ice concentration is achieved by Sentinel-1 (Fig. 5).

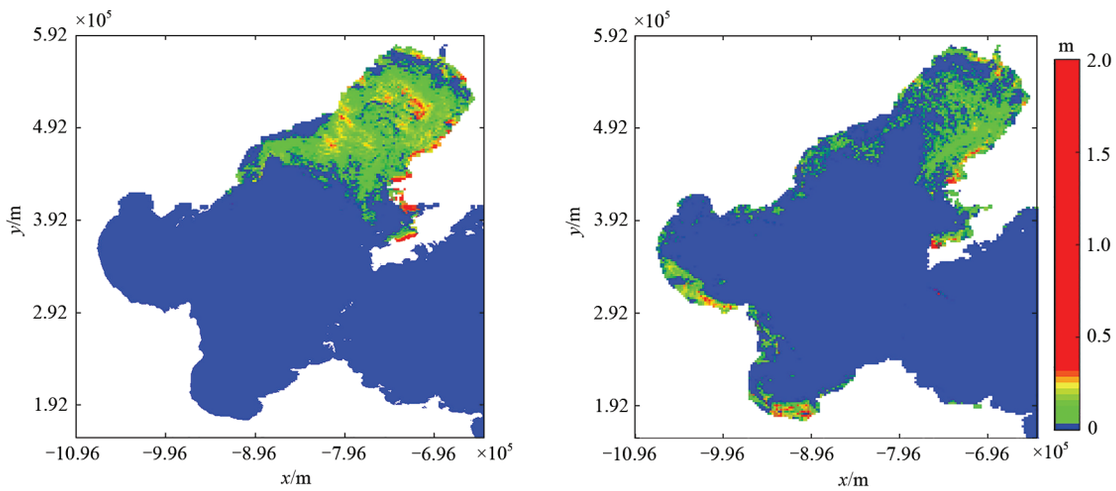

(a) 2013-02-08 (b) 2016-02-02

Fig.4 Sea-ice thickness results by GOCI

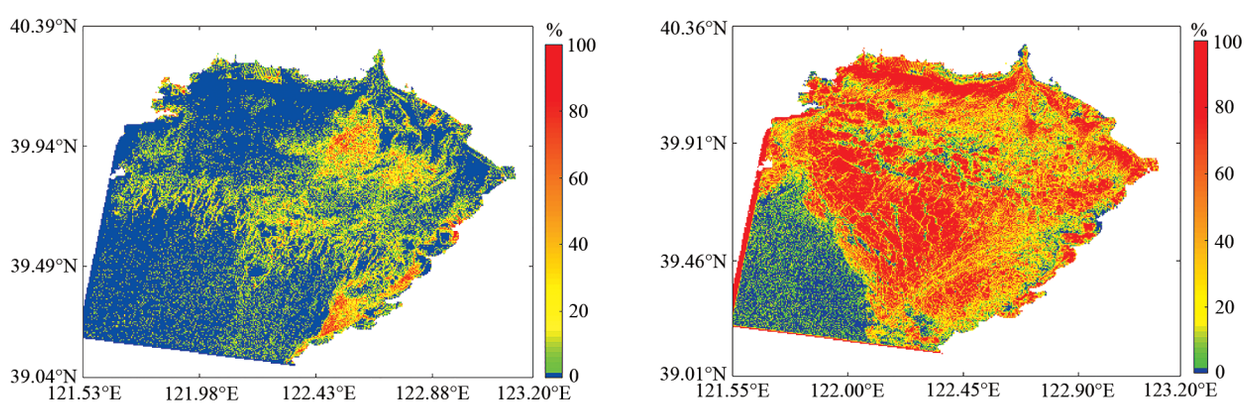

(a) 2016-01-06 (b) 2016-01-28

Fig.5 Sea-ice concentration results by Sentinel-1

(2) *Sea-ice concentration calculated by GOCI*

The sea ice and the sea water can be recognized by the sea-ice thickness results using GOCI data in the previous section. All pixels bigger than 0 in the sea-ice thickness results of the COCI images are set to 1, which represent the sea ice. The other pixels are set to 0. Then, the sea-ice concentration of one pixel is set to be the mean value of the pixels surrounding this pixel within the 3 × 3 window (Fig. 6 in Orthographic projection, unit: m).

3.3 Sea-ice velocity

The sea-ice velocity (V_i) is extracted using the GOCI images, which employs the Maximum Cross-correlation (MCC) method for daily 1-hour sea ice drift tracking in the Bohai Sea. The sea ice drift monitoring is accomplished by tracking the distinct characteristics of sea ice samples (Wu, 2014; Lang, *et al*., 2014). Assume that the A and B images are obtained at sequential time of t_1 and t_2, respectively. For each sea-ice fragment with typical features at point $P_1(x_1, y_1)$ in the A image, the best matching fragment with the same size is found at point $P_2(x_2, y_2)$ in the B image using the MCC method. According to the location drift in the two images, the drift speed components can be calculated as follows

$$v_x = (x_2 - x_1) \times 500 / (3600 \times h) \text{ (unit: m/s)} \quad (3a)$$

$$v_y = (y_2 - y_1) \times 500 / (3600 \times h) \text{ (unit: m/s)} \quad (3b)$$

where x_i and y_i (i =1,2) represent the eastward and northward components of the image coordinates (pixels), respectively; v_x and v_y represent the eastward and northward components of the sea-ice velocity, respectively; and h is the time delay (t_2 - t_1) between the two images. The results are shown in Fig. 7 in Orthographic projection (unit: m).

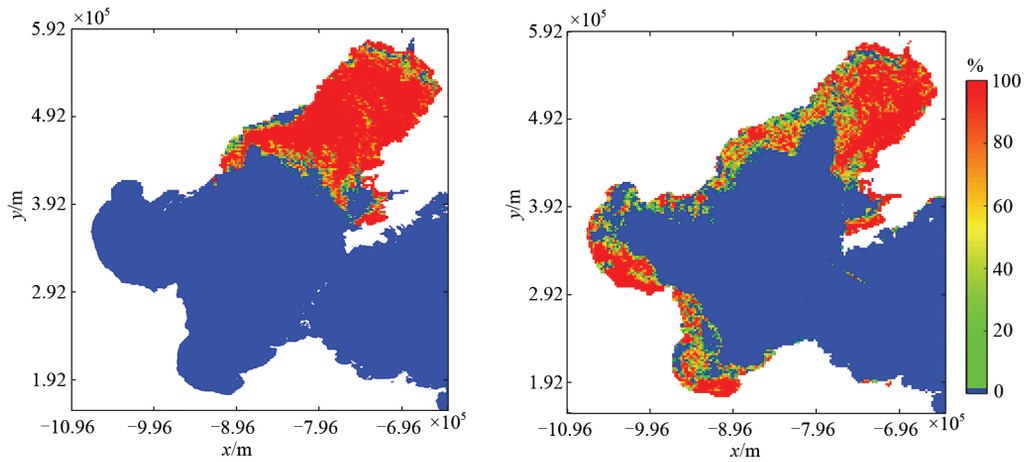

(a) 2013-02-08 (b) 2016-02-02

Fig.6 Sea-ice concentration results by GOCI

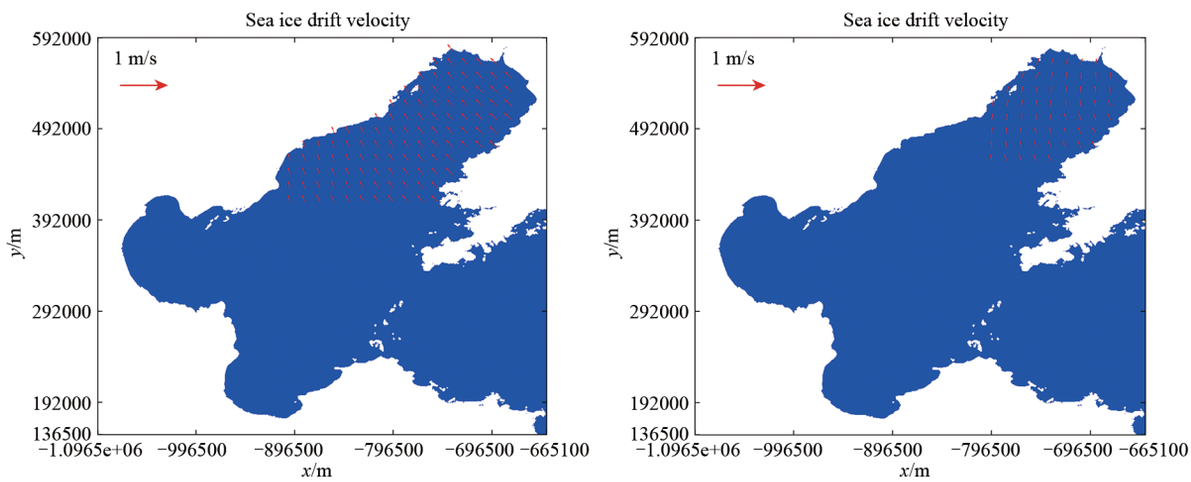

(a) 2013-02-28 (b) 2016-02-02

Fig.7 Sea-ice velocity results by GOCI

4 SEA-ICE-HAZARD EVALUATION

The different sea-ice-hazard indexes should be defined for different disaster-bearing bodies of the marine transportation and the offshore constructions. Based on the sea-ice parameters of the concentration, thickness, and velocity, the two types of the sea-ice-hazard indexes are calculated, used to evaluate the spatial distribution features and the inter-annual variations of the sea-ice disaster quantitatively in the Bohai Sea in the period from 2011 to 2017.

4.1 For the marine transportation (I_1)

If the sea-ice concentration and thickness are larger, the sea-ice breaking is harder, which causes blocking the marine transportation severely. The sea-ice influence for the marine transportation focused on the sea-ice volume which is equal to multiplying the sea-ice concentration (C_i) by the sea-ice thickness (H_i), which is indicated the sea-ice mass per unit area in physics. Therefore, the sea-ice-hazard index for the marine transportation is represented by the sea-ice volume, which is defined by I_1

$$I_1 = C_i \times H_i \text{ (unit: \%·m)} \quad (4)$$

where, the larger value of I_1 means less navigable. According to the grades of the sea-ice parameters, the sea-ice-hazard index for the marine transportation can be also divided into four grades, shown in Table 2. The distribution of I_1 are shown in Fig. 8 in Orthographic projection (unit: m).

Table 2 The grades of the sea-ice-hazard index for the marine transportation

unit	Grade 1	Grade 2	Grade 3	Grade 4
	Non hazard	Low hazard	Mild hazard	Severe hazard
%·m	0—1.5	1.5—10	10—24	>24

4.2 For the offshore constructions (I_2)

If the sea-ice volume and velocity are larger, the sea ice has a greater impact on the offshore constructions (e.g. the oil platform), which leads to large loss. The sea-ice influence for the offshore constructions focused on the combined action of the sea-ice volume and velocity which is the sea-ice concentration (C_i) times the sea-ice thickness (H_i) times the sea-ice velocity (V_i), which is indicated the sea-ice momentum per unit area in physics. Therefore, the sea-ice-hazard index for the offshore constructions is represented by the sea-ice momentum, which is defined by I_2

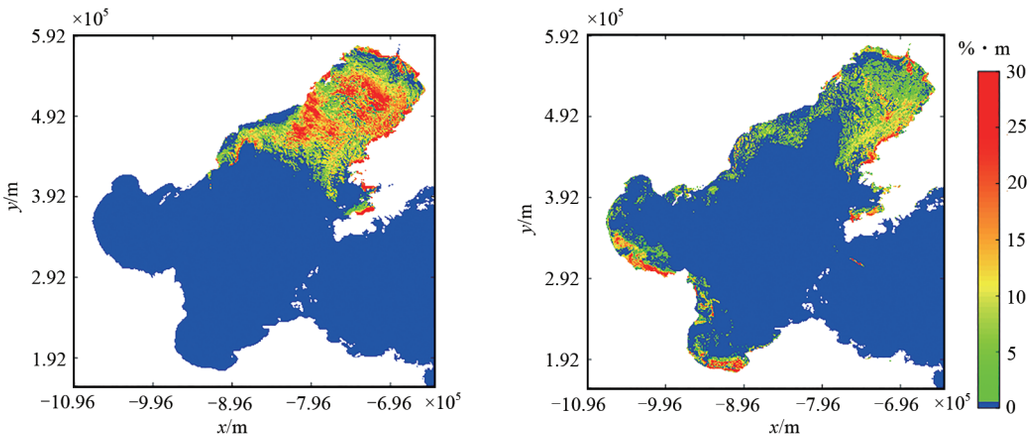

(a) 2013-02-08 (b) 2016-02-02

Fig.8 Sea-ice-hazard index for the marine transportation

$$I_2 = I_1 \times V_i = C_i \times H_i \times V_i \text{ (unit: \%·m}^2\text{·s}^{-1}\text{)} \quad (5)$$

where, the bigger value of I_2 means a higher extruding pressure and impulse force imposed by the sea ice. According to the grades of the sea-ice parameters, the sea-ice-hazard index for the offshore constructions can also be divided into four grades, shown in Table 3. The distribution of I_2 are shown in Fig. 9 in Orthographic projection (unit: m).

Table 3 The grades of the sea-ice-hazard index for the offshore constructions

unit	Grade 1 Non hazard	Grade 2 Low hazard	Grade 3 Mild hazard	Grade 4 Severe hazard
%·m²·s⁻¹	0—0.3	0.3—4	4—14.4	>14.4

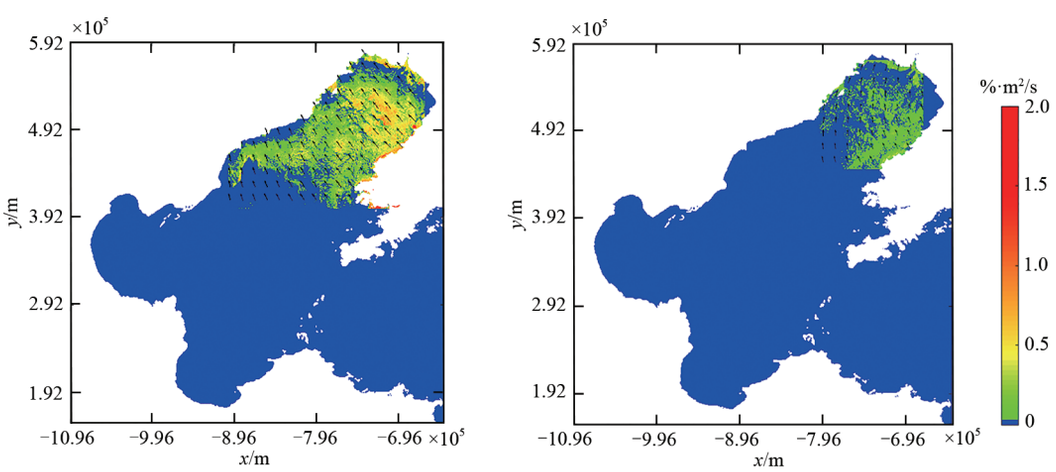

(a) 2013-02-08 (b) 2016-02-02

Fig.9 Sea-ice-hazard index for the offshore constructions

4.3 The analysis on sea-ice disaster

(1) *Annual analysis*

According to the sea-ice-hazard indexes for the marine transportation and the offshore constructions from 2011 to 2017, the variability and their features of the sea-ice disaster distribution in the Bohai Sea are analyzed. It is found that the sea-ice-hazard indexes is often smaller in the November and December, then increases from January to February. Finally, the sea ice disappears in March. The characteristics of the sea-ice-hazard indexes of 2015\2016 were taken for an example shown in Fig. 10.

(2) *Inter-annual analysis*

According to the sea-ice-hazard indexes for the marine transportation and the offshore constructions, the changes and their features of the sea-ice disaster distribution are analyzed in the Bohai Sea from 2011 to 2017. The sea-ice-hazard indexes are bigger in the 2012\2013 and 2015\2016, milder in the 2011\2012 and 2014\2015, and lighter in the 2013\2014 and 2016\2017, shown in Fig. 11.

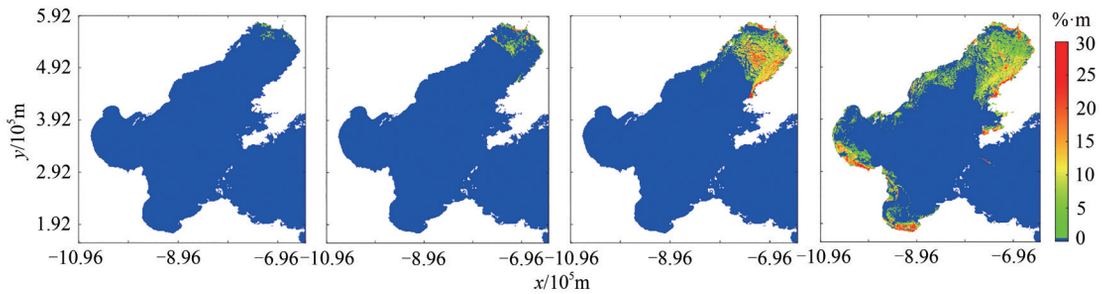

(a) 2015-12-27 (I_1) (b)2016-01-09 (I_1) (c)2016-01-19 (I_1) (d)2016-02-02 (I_1)

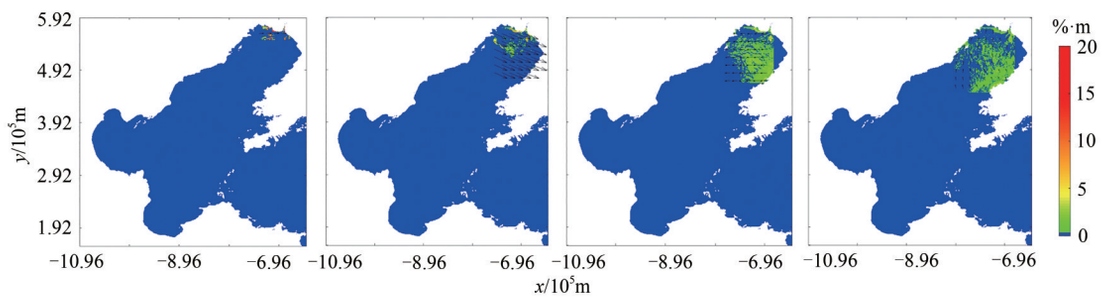

(a) 2015-12-27 (I_2) (b)2016-01-09 (I_2) (c)2016-01-19 (I_2) (d)2016-02-02 (I_2)

Fig.10 Sea-ice Disaster analysis in 2015/2016

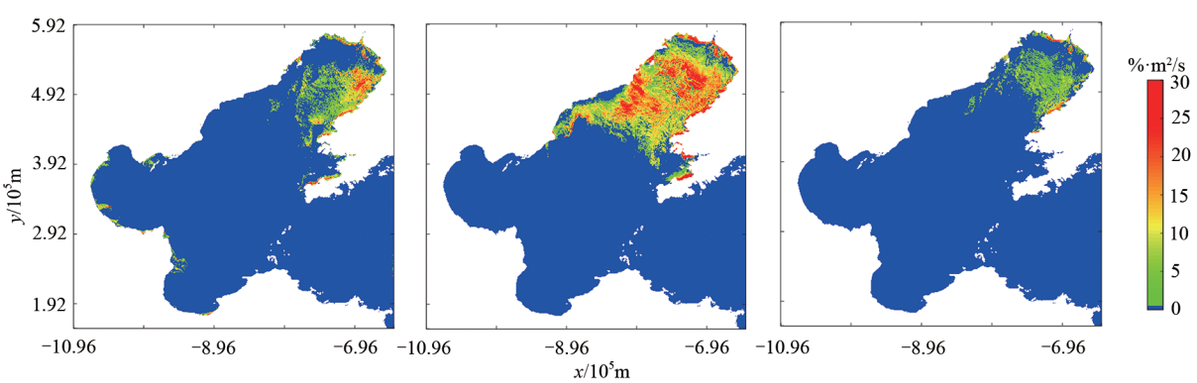

(a) 2012-02-18 (I_1) (b) 2013-02-08 (I_1) (c) 2014-02-10 (I_1)

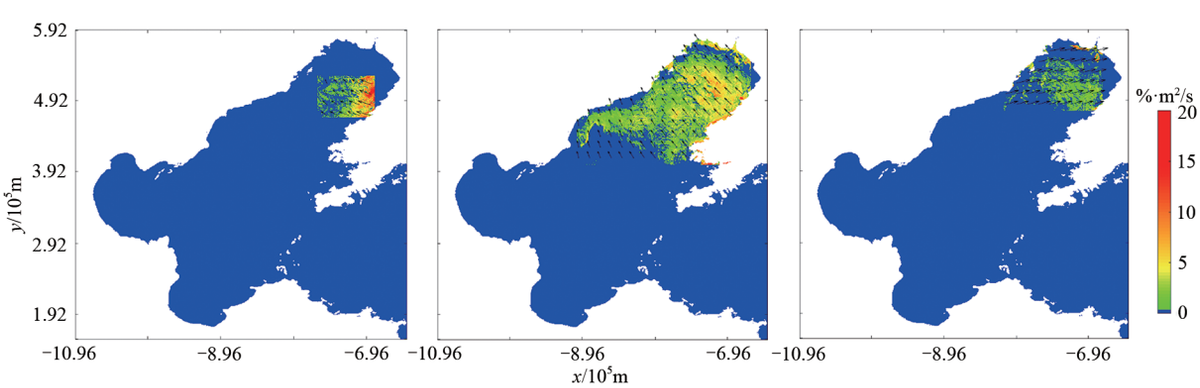

(d) 2012-02-18 (I_2) (e) 2013-02-08(I_2) (f) 2014-02-10 (I_2)

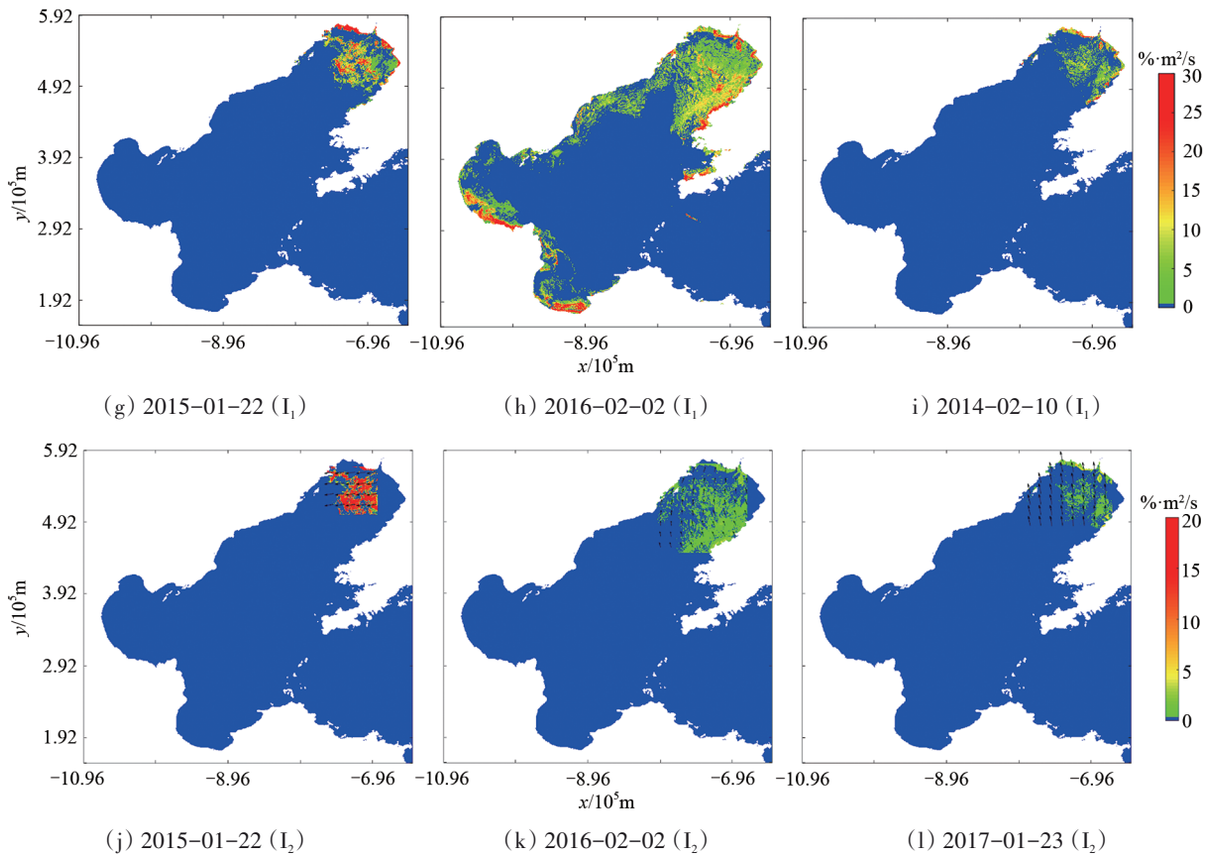

Fig.11 Sea−ice Disaster analysis from 2011 to 2017

5 CONCLUSION

In the Dragon-4 programme, the sea-ice-hazard indexes, for the marine transportation (I_1) and the offshore constructions (I_2) respectively, are used to eualuate quantitatively the space-time distribution features of the sea-ice disaster in the Bohai Sea from 2011—2017, which can satisfy the requests of the sea-ice disaster prevention and reduction and provide references to the monitoring and research on the sea-ice disaster.

Acknowledgment: This work was ceiried out as part of the Dragon-4 Programme (No. 32292) by the Ministry of science and Technology of the P.R.china and the Earopean space Agency.

REFERENCES

Grenfell T C, Perovich D K. 1984. Spectral albedos of sea ice and incident solar irradiance in the southern Beaufort Sea [J]. Journal of Geophysical Research: Oceans (1978–2012), 89(C3: 3573-3580.

Gu W, Liu C, Yuan S, Li N, Chao J L, Li L T and Xu Y G. 2013. Spatial distribution characteristics of sea-ice-hazard risk in Bohai, China. Annals of Glaciology, 54(62): 73-79. https://sentinel. esa. int/web/sentinel/missions/sentinel-1, 2016.

Kim M, Kim J, Wong M S, Yoon J, Lee J, Wu D, Chan P W, Nichol J E, Chung C-Y and Ou M-L. 2014. Improvement of aerosol optical depth retrieval over Hong Kong from a geostationary meteorological satellite using critical reflectance with background optical depth correction[J]. Remote Sensing of Environment, 142: 176-187.

Lang W, Wu Q, Zhang X, Meng J, Wang N and Cao Y J. 2014. Sea ice drift tracking in the Bohai Sea using geostationary ocean color imagery[J]. Journal of Applied Remote Sensing, 8(1):083650.

Liu M, Dai Y, Zhang J, Zhang X and Meng J. 2013. The research on the object-based method of sea ice classification of high-resolution quad-polarization SAR data. Acta Oceanologica Sinica (in Chinese), 35(4): 80-87.

Liu M, Dai Y, Zhang J, Zhang X and Meng J. 2014. First-year level sea-ice thickness retrieval in Labrador Sea using C-band polarimetric SAR data. Journal of China University of Petroleum (in Chinese), 38(3): 186-192.

Liu M, Dai Y, Zhang J, Zhang X and Meng J. 2015. PCA-based sea-ice image fusion of optical data by HIS transform and SAR data by wavelet transform. Acta Oceanologica Sinica, 34(3): 59-67

Liu M, Dai Y, Zhang J, Zhang X and Meng J. 2015. PCA-based sea-ice image fusion of optical data by HIS transform and SAR data by wavelet transform. Acta Oceanologica Sinica, 34(3): 59-67.

Liu Wensong, Sheng Hui, Zhang Xi. 2016. Sea ice thickness estimation in the Bohai Sea using geostationary ocean color imager data[J]. Acta Oceanologica Sinica, 35(7): 105-112.

Liu Wensong. 2016. Research on Sea-ice Parameters Retrieval Based on Active and Passive Remote Sensing Data in the Bohai Sea[D]. Qingdao: China University of Petroleum Degree Thesis of Engineering Master.

Luo Y, Wu H, Zhang Y, Sun C and Liu Y. 2004. Application of the HY-1 satellite to sea ice monitoring and forecasting. Acta Oceanologica Sinica, 23(2): 251-266.

Ryu J H, Han H J, Cho S, Park Y J and Ahn Y H. 2012. Overview of geostationary ocean color imager (GOCI) and GOCI data processing system (GDPS)[J]. Ocean Science Journal, 47(3): 223-233.

Shi W, Wang M. 2012a. Sea ice properties in the Bohai Sea measured by MODIS-Aqua: 1. satellite algorithm development[J]. Journal

of Marine Systems, 95: 32-40

Shi W, Wang M. 2012b. Sea ice properties in the Bohai Sea measured by MODIS-Aqua: 2. Study of sea ice seasonal and interannual variability[J]. Journal of Marine Systems, 95(1): 41-49.

Su H, Wang Y, Yang J. 2012. Monitoring the spatiotemporal evolution of sea ice in the Bohai Sea in the 2009–2010 winter combining MODIS and meteorological data. Estuaries and Coasts, 35: 281–291.

Su H, Wang Y. 2012a. Using MODIS data to estimate sea ice thickness in the Bohai Sea (China) in the 2009–2010 winter. Journal of Geophysical Research, 117: C10018

Su H, Wang Y. 2012b, Estimating sea ice thickness using MODIS data: a case study in the Bohai Sea, China. In: Proceedings of the 2012 Second International Workshop on Earth Observation and Remote Sensing Applications (EORSA). Shanghai: 111–115

Wu L, Wu H, Sun L, Zhang Y, Liu Y and Wei X. 2006. Retrieval of sea ice in the Bohai Sea from MODIS data. Periodical of Ocean University of China (in Chinese), 36(2): 173–179.

Wu Qing. 2014. Sea Ice Drift Tracking in the Bohai Sea Based on GOCI[D]. Hefei: Hefei University of Technology.

Xie F, Gu W, Ha S, Cui W, Chen W, Zhou C, Huang S and Liu Z. 2006. An experimental study on the spectral characteristics of one year-old sea ice in the Bohai Sea, China. International Journal of Remote Sensing, 27(14): 3057–3063.

Xu Z, Yang Y, Sun Z, Li Z, Cao W and Ye H. 2012. In situ measurement of the solar radiance distribution within sea ice in Liaodong Bay, China. Cold Regions Science and Technology, 71: 23–33.

Yang G. 2000. Engineering of Sea Ice (in Chinese). Beijing: Petroleum Industry Press, 596.

Yuan S, Gu W, Xu Y, Wang P, Huang S, Le Z and Cong J. 2012. The estimate of sea ice resources quantity in the Bohai Sea based on NOAA/AVHRR data. Acta Oceanologica Sinica, 31(1): 33–40.

Zhang X, Zhang J, Meng, Junmin. 2016. Techniques for Sea Ice Characteristics Extraction and Sea Ice Monitoring Using Multi-Sensor Satellite Data in the Bohai Sea, Dragon 3 Programme Final Report (2012-2016[C]// Dragon 3 Final Results and Dragon 4 Kick-Off. Dragon 3 Final Results and Dragon 4 Kick-Off, 2016.

Zhang Y, Zhang M, Ji Y. 2016. Sea Ice Detection with Sentinel-1A Dual Polarization SAR Data[C]// Dragon 3 Final Results and Dragon 4 Kick-Off. Dragon 3 Final Results and Dragon 4 Kick-Off, 2016.